

Tetrolets-based System for Automatic Skeletal Bone Age Assessment

Dr.P.Thangam¹, Dr.T.V.Mahendiran²

¹Associate Professor, CSE Department, Coimbatore Institute of Engineering and Technology, India

²Associate Professor, EEE Department, Coimbatore Institute of Engineering and Technology, India

ABSTRACT:

This paper presents the design and implementation of the tetrolets based system for automatic skeletal Bone Age Assessment (BAA). The system works according to the renowned Tanner and Whitehouse (TW2) method, based on the carpal and phalangeal Region of Interest (ROI). The system ensures accurate and robust BAA for the age range 0-10 years for both girls and boys. Given a left hand-wrist radiograph as input, the system estimates the bone age by deploying novel techniques for segmentation, feature extraction, feature selection and classification. Tetrolets are used in combination with Particle Swarm Optimization (PSO) for segmentation. From the segmented wrist bones, the carpal and phalangeal ROI are identified and are used in morphological feature extraction. PCA is employed as a feature selection tool to reduce the size of the feature vector. The selected features are fed in to an ID3 decision tree classifier, which outputs the class to which the radiograph is categorized, which is mapped onto the final bone age. The system was evaluated on a set of 100 radiographs (50 for girls and 50 for boys), and the results are discussed. The performance of system was evaluated with the help of radiologist expert diagnoses. The system is very reliable with minimum human intervention, yielding excellent results.

Keywords: Bone Age Assessment (BAA), TW2, radiograph, Particle Swarm Optimization (PSO), Tetrolets, ID3, Classification.

1. Introduction:

The chronological situations of humans are described by certain indices such as height, dental age, and bone maturity. Of these, bone age measurement plays a significant role because of its reliability and practicability in diagnosing hereditary diseases and growth disorders. Bone age assessment using a hand radiograph is an important clinical tool in the area of pediatrics, especially in relation to endocrinological problems and growth disorders. A single reading of skeletal age informs the clinician of the relative maturity of a patient at a particular time in his or her life and integrated with other clinical finding, separates the

normal from the relatively advanced or retarded [1]. The bone age of children is apparently influenced by gender, race, nutrition status, living environments and social resources, etc. Based on a radiological examination of skeletal development of the left-hand wrist, bone age is assessed and compared with the chronological age. A discrepancy between these two values indicates abnormalities in skeletal development. The procedure is often used in the management and diagnosis of endocrine disorders and also serves as an indication of the therapeutic effect of treatment. It indicates whether the growth of a patient is accelerating or decreasing, based on which the patient can be treated with growth hormones. BAA is universally used due to its simplicity, minimal radiation exposure, and the availability of multiple ossification centers for evaluation of maturity.

2. Background of BAA:

The main clinical methods for skeletal bone age estimation are the Greulich & Pyle (GP) method and the Tanner & Whitehouse (TW) method. GP is an atlas matching method while TW is a score assigning method [2]. GP method is faster and easier to use than the TW method. Bull et. al. performed a large scale comparison of the GP and TW method and concluded that TW method is the more reproducible of the two and potentially more accurate [3].

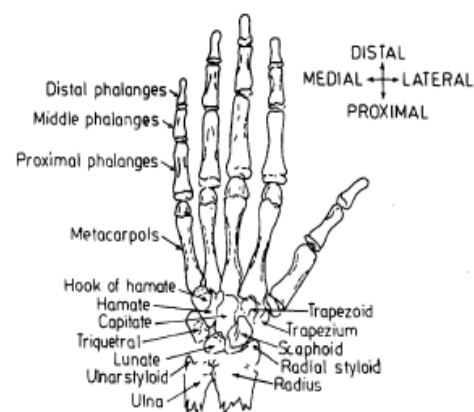


Fig. 1. Bones of hand and wrist for BAA

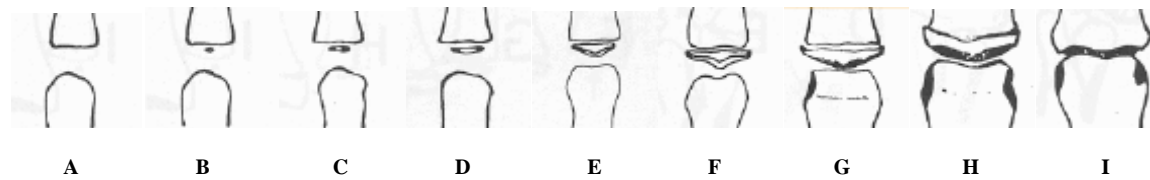


Fig. 2. TW stages for phalanx bone

In GP method, a left-hand wrist radiograph is compared with a series of radiographs grouped in the atlas according to age and sex. The atlas pattern which superficially appears to resemble the clinical image is selected. Since each atlas pattern is assigned to a certain year of age, the selection assesses the bone age. The disadvantage of this method is the subjective nature of the analysis performed by various observers with different levels of training. The reason for high discrepancies in atlas matching method is due to a general comparison of the radiograph to the atlas pattern. By a more detailed comparison of individual bones, ambiguous results may be obtained.

TW method uses a detailed analysis of each individual bone (shown in Fig. 1), assigning it to one of eight classes reflecting its developmental stage. This leads to the description of each bone in terms of scores. The sum of all scores assesses the bone age. This method yields the most reliable results. The high complexity of the TW method is the main reason for its less intensive use and what makes it worthwhile to automate. The original Tanner-Whitehouse method (TW1, 1962) was presented by Tanner, Whitehouse and Healy. The fundamental advantage of TW1 was its solid and formal mathematical soul. Based on stages, scores were assigned and later on added to obtain the final skeletal age. TW2 was a revision of TW1, especially in relation to the scores associated to each stage and also the difference between both sexes. The TW2 method does not use a scale based on the age, rather it is based on a set of bone's standard maturity for each age population. In detail, in the TW2 method twenty regions of interest (ROIs), located in the main bones are considered for the bone age evaluation. Each ROI is divided into three parts: Epiphysis, Metaphysis and Diaphysis; it is possible to identify these different ossification centers in the phalanx proximity. The development of each ROI is divided into discrete stages, as shown in Fig. 2, and each stage is given a letter (A,B,C,D,...I), reflecting the development stage as:

- Stage A – absent
- Stage B – single deposit of calcium
- Stage C – center is distinct in appearance

- Stage D – maximum diameter is half or more the width of metaphysis
- Stage E – border of the epiphysis is concave
- Stage F – epiphysis is as wide as metaphysis
- Stage G – epiphysis caps the metaphysis
- Stage H – fusion of epiphysis and metaphysis has begun
- Stage I – epiphyseal fusion completed.

By adding the scores of all ROIs, an overall maturity score is obtained. This score is correlated with the bone age differently for males and females [4]. For TW2 method, these score systems have been developed:

- TW2 20 bones: characterized by 20 bones including the bones of the first, third and fifth finger and the carpal bones.
- RUS: considers the same bones of the TW2 method except the carpal bones.
- CARPAL: considers only the carpal bones.

A number of algorithms for automated skeletal bone age assessment exist in the literature.

3. Survey of Literature:

In early 1980s, Pal and King proposed the theory of fuzzy sets and applied it for edge detection algorithm of X-ray images [5]. Kwabwe et. al. later in 1986, proposed certain algorithms to recognize the bones in an X-ray image of the hand and wrist [6]. They used a shape description technique based on linear measurements from a polygonal approximation of the bones. A fuzzy classifier for syntactic recognition of different stages of maturity of bones from X-rays of hand and wrist using fuzzy grammar and fuzzy primitives was developed by Pathak and Pal [7]. It comprised of a hierarchical three-stage syntactic recognition algorithm, which made use of six-tuple fuzzy and seven-tuple fractionally fuzzy grammars to identify the different stages of maturity of bones from X-rays. Michael and Nelson [8] developed a model-based system for automatic segmentation of bones from digital hand radiographs named as HANDX, in 1989. This computer vision system, offered a solution to automatically find, isolate and measure bones from digital X-rays. In 1991, Pietka et. al. described a method [9] based on independent analysis of the phalangeal regions. Phalangeal analysis was performed in several

stages by measuring the lengths of the distal, middle and proximal phalanx. These measurements were converted into skeletal age by using the standard phalangeal length table proposed by Garn et.al [10]. These single bone age estimates were then averaged to assess the global phalangeal age of the patient.

Tanner and Gibbons introduced the Computer-Assisted Skeletal Age Scores (CASAS) system in 1992 [11]. This was based on nine prototype images for each bone, representing the nine stages of maturity. Thus, a stage was defined by an image template. Two or three most similar templates for the radiographs were identified. The system then automatically computed a measure of correlation to each template and a fractional stage. The correlation to the template was a measure of similarity. In 1993, Pietka et. al. performed phalangeal and carpal bone analysis using standard and dynamic thresholding methods to assess skeletal age [12]. Cheng et. al. [13] proposed the methods to extract a region of interest (ROI) for texture analysis in 1994, with particular attention to patients with hyperparathyroidism. The techniques included multiresolution sensing, automatic adaptive thresholding, detection of orientation angle, and projection taken perpendicular to the line of least second moment. In the same year, Drayer and Cox [14] designed a computer aided system to estimate bone age based on Fourier analysis on radiographs to produce TW2 standards for radius, ulna and short finger bones. It employed template matching of each bone to the scanned image of the radiograph. In 1996, Al-Taani et. al. classified the bones of the hand-wrist images into pediatric stages of maturity using Point Distribution Models (PDM) [15]. Wastl and Dickhaus proposed a pattern recognition based BAA approach, in the same year [16]. The approach consisted of four major steps: digitization of the hand radiograph, segmentation of ROI, prototype matching and BAA. In 1999, Bull et. al. made a remarkable comparison of GP and TW2 methods [3] and concluded the following. The GP method involves a complex comparison of all of the bones in the hand and wrist against reference "normal" radiographs of different ages. Although this approach is considerably faster than the original, it may be less accurate. The TW2 method relies on the systematic evaluation of the maturity of all the bones in the hand and wrist. The measured intra-observer variation was greater for the GP method than for the TW2 method. This accounts for much of the discrepancy between the two methods. They also concluded that the GP and TW2 methods produce different values for bone age, which are significant in clinical practice. They have also shown that the TW2 method is more reproducible than

the GP method. They finally suggested TW2 method to be preferably used as the only one BAA method when performing serial measurements of a patient. Mahmoodi et. al. (1997) used Knowledge-based Active Shape Models (ASM) in an automated vision system to assess the bone age [17]. Pietka et. al. conducted a computer assisted BAA procedure [18] by extracting and using the epiphyseal/ metaphyseal ROI (EMROI), in 2001. From each phalanx 3 EMROIs were extracted which include: metaphysis, epiphysis and diaphysis of the distal and middle phalanges and for the proximal phalanges it includes metaphysis, epiphysis and upper part of metacarpals of proximal phalanges. The diameters of metaphysis, epiphysis and diaphysis of each EMROI were measured. The extracted features described the stage of skeletal development more objectively than visual comparison. Niemeijer et. al. automated the TW method to assess the skeletal age from a hand radiograph [19]. They employed an ASM segmentation method developed by Cootes and Taylor [20] to segment the outline of the bones. Then the mean image for an ROI in each TW2 stage was constructed. Next, an ASM was developed to determine the shape and location of the bones in a query ROI, so that this ROI can be aligned with each of the mean images in the third step. Then the correlation between a fixed area around the bones in the mean images and the query ROI was computed. These correlation coefficients were used to determine the TW2 stage in the final step.

M.Fernandez et. al. [21] described a method for registering human hand radiographs for automatic BAA using the GP method. This method was the first step towards a segmentation-by-registration procedure to carry out a detailed shape analysis of the bones of the hand. Accurate results were obtained at a fairly low computational load. A.Fernandez et. al. proposed a fuzzy logic based neural architecture for BAA [22]. The system employed a computing with words paradigm, wherein the TW3 statements were directly used to build the computational classifier. Luis Garcia et. al. presented a fully automatic algorithm [23] to detect bone contours from hand radiographs using active contours. Lin et. al. proposed a novel and effective carpal bone image segmentation method using GVF model, to extract a variety of carpal bone features [24]. In 2005, Tristan and Arribas [25] designed an end-to-end system to partially automate the TW3 bone age assessment procedure, using a modified K-means adaptive clustering algorithm for segmentation, extracting up to 89 features and employing LDA for feature selection and finally estimating bone age using a Generalized Softmax Perceptron (GSP) NN, whose optimal complexity was estimated via the Posterior

Probability Model Selection (PPMS) algorithm. Zhang et. al. developed a knowledge based carpal ROI analysis method [26] for fully automatic carpal bone segmentation and feature analysis for bone age assessment by fuzzy classification. Thodberg et. al. proposed a 100% automated approach called the Bone Xpert method [27]. The architecture of Bone Xpert divided the processing into three layers: Layer A to reconstruct the bone borders, Layer B to compute an intrinsic bone age value for each bone and Layer C to transform the intrinsic bone age value using a relatively simple post-processing. Giordano et. al. [28] designed an automated system for skeletal bone age evaluation using DoG filtering. The bones in the EMROIs, were extracted using the DoG filter and enhanced using a novel adaptive thresholding obtained by histogram processing. Finally, the main features of these bones were extracted for TW2 evaluation. Hsieh et. al. [29] proposed an automatic bone age estimation system based on the phalanx geometric characteristics and carpal fuzzy information. From the phalanx ROI and carpal ROI, features were extracted and classified as phalanx bone age and carpal bone age respectively. Classification employed back propagation, radial basic function and SVM neural networks to classify phalanx bone age. Normalized bone age ratio of carpals was used to compute the fuzzy bone age. Zhao Liu and Jian Liu proposed an automatic BAA method with template matching [30] based on PSO. An edge set model was designed to store the middle information of image edge detection. The image template matching was based on PSO, followed by classification. TW3 classifier proposed by A.Fernandez et. al. (discussed in section 3.17) was made use of to obtain the bone age. Giordano et. al [31] presented an automatic system for BAA using TW2 method by integrating two systems: the first using the finger bones – EMROI and the second using the wrist bones – CROI. Then the TW2 stage is assigned by combining Gradient Vector Flow (GVF) Snakes and derivative difference of Gaussian filter. We have presented a thorough survey of literature on BAA methods in our previous work [32], explaining in detail the various work done in BAA and providing directions for future research. Our previous work [33] describes a computerized BAA method for carpal bones, by extracting features from the convex hull of each carpal bone, named as the convex hull approach. We have also proposed an automated BAA method to estimate bone age from the feature ratios extracted from carpal and radius bones, named as the feature ratio approach [34]. Our decision tree approach utilizes features from the radius and ulna bones and their epiphyses for BAA [35]. We have also exploited the epiphysis/ metaphysis

region of interest (EMROI) in BAA using our Hausdorff distance approach [36].

4. The Proposed system:

The proposed system consists of two phases, namely: the Training phase (Fig. 3) and the Testing phase (Fig.4). Both the phases share the following modules:

- Image Pre-processing
- Morphological Feature Extraction
- Feature Analysis and Selection

The last module of the training phase is the

- Training Module (to train the ID3 classifier)

The last module of the testing phase is the

- Testing Module (to classify the image into its age class, thus inferring the bone age).

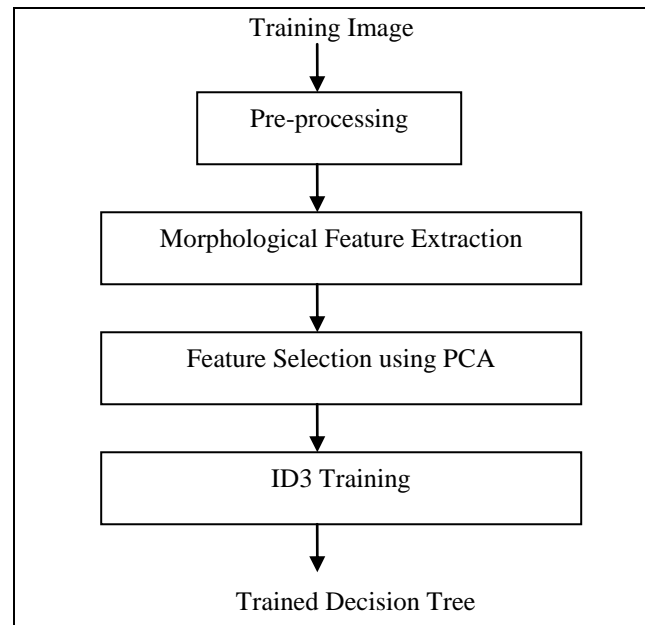
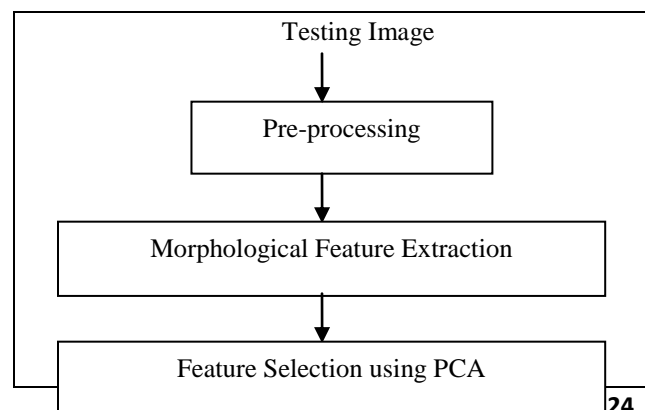


Fig. 3. Training Phase



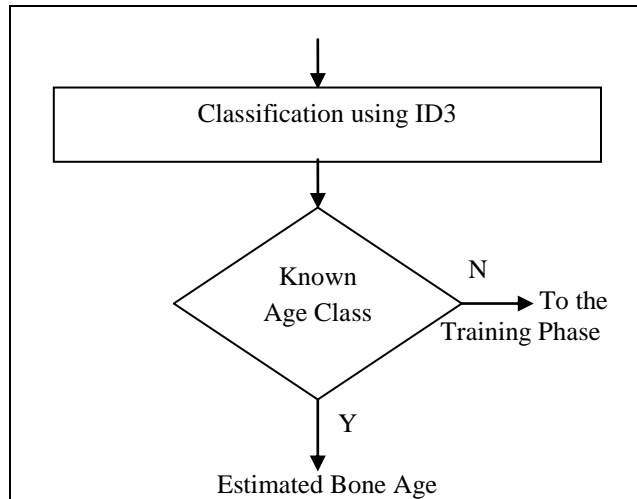


Fig. 4. Testing Phase

4.1 Image Pre-processing

Image preprocessing is performed in two steps:

1. Image Enhancement
2. PSO-Segmentation using Tetrolets

The input image is enhanced by image smoothing to reduce the noise within the image or to produce a less pixilated image. In our system, we have done smoothing using a Gaussian filter to reduce noise.

4.1.1 Edge Detection and Segmentation

We have made use of Sobel edge detector to detect the edges. The Sobel edge detector uses a pair of 3 x 3 convolution masks, one estimating the gradient in the x-direction (columns) and the other estimating the gradient in the y-direction (rows). A convolution mask is usually much smaller than the actual image. As a result, the mask is slid over the image, manipulating a square of pixels at a time.

Tetrolet-based segmentation method proposed in this paper, makes use of tetrolets for decomposing the input image into sparse representation. The decomposed tetrolet co-efficients [38] are fed as particle solutions to the PSO segmentation algorithm. The algorithm segments the input left hand wrist radiograph and identifies the ROIs for further computations.

4.1.2 Decomposition into Tetrolets:

1. The image a^{r-1} is divide into blocks $Q_{i,j}$ of size 4×4 , $i, j = 0, \dots, N/4^r - 1$.
2. In each block $Q_{i,j}$, the 117 admissible tetromino coverings $c = 1, \dots, 117$ are considered.

For each tiling c , a Haar wavelet transform is applied to the four tetromino subsets $I_s^{(c)}$, $s = 0, 1, 2, 3$. In this

way, for each tiling c , four low-pass coefficients and 12 tetrolet coefficients are obtained. In $Q_{i,j}$, the pixel averages for every admissible tetromino configuration $c = 1, \dots, 117$ by equation (3) and the three high-pass parts for $i = 1, 2, 3$ given by equation (4) respectively:

$$a^{r,(c)} = (a^{r,(c)}[s])_{s=0}^3 \text{ with } a^{r,(c)}[s] = \sum_{(m,n) \in I_s^{(c)}} \varepsilon[0, L(m,n)] a^{r-1}[m,n] \quad (3)$$

$$w_i^{r,(c)} = (w_i^{r,(c)}[s])_{s=0}^3 \text{ with } w_i^{r,(c)}[s] = \sum_{(m,n) \in I_s^{(c)}} \varepsilon[i, L(m,n)] a^{r-1}[m,n] \quad (4)$$

where the coefficients $\varepsilon[l,m]$, $l,m = 0, \dots, 3$, are entries from the Haar wavelet transform matrix:

$$W := (\varepsilon[l, m])_{l,m=0}^3 = \frac{1}{2} \begin{pmatrix} 1 & 1 & 1 & 1 \\ 1 & 1 & -1 & -1 \\ 1 & -1 & 1 & -1 \\ 1 & -1 & -1 & 1 \end{pmatrix} \quad (5)$$

3. The low- and high-pass coefficients of each block are re-arranged into a 2 x 2 block.
4. The tetrolet coefficients (high-pass part) are stored.
5. Step 1 to 4 is applied to the low-pass image.
6. The tetrolet coefficients are fed as input to the PSO algorithm for segmentation.

4.1.3 Overview of PSO:

Particle Swarm Optimization (PSO) is an algorithm for finding optimal regions of complex search space through interaction of individuals in a population of particles. PSO algorithm, originally introduced in terms of social and cognitive behavior by Eberhart and Kennedy [39] has been proven to be a powerful competitor to other evolutionary algorithms such as genetic algorithms. PSO is a population based stochastic optimization technique and well adapted to the optimization of nonlinear functions in multidimensional space [40]. PSO algorithm simulates social behavior among individuals (particles) flying through multidimensional search space, each particle representing a single intersection of all search dimensions [41]. The particles evaluate their positions relative to a global fitness at every iteration, and companion particles share memories of their best positions, and then use those memories to adjust their own velocities and positions. At each generation, the velocity of each particle is updated, being pulled in the direction of its own previous best solution (local) and the best of all positions (global) [42,43]. Computation of optimal threshold is handled here with Particle Swarm Optimization (PSO). There are six important control parameters in PSO algorithm. They are: Population

Size, Cognitive Learning Rate, Social Learning Rate, Maximum of Particle Flying Speed, Inertia Weight factor, and Constriction factor. The population size of particles refers the number of particles in iterative process, thus denoting components in the image here. A population of particles is initialized with random positions and velocities in d-dimensional space. A fitness function, f is evaluated, using the particle's positional coordinates as input values. Positions and velocities are adjusted, and the function is evaluated with the new coordinates at each time-step.

Algorithm

Step 1: In every iteration, each particle is updated by following two "best" values, Personal best and Global best.

Step 2: After finding the two best values, the particle updates its velocity and positions with following equation (6) and (7)

$$v[i] = v[i] + c1 * rand(i) * (pbest[i] - present[i]) + c2 * rand(i) * (gbest[i] - present[i]) \quad (6)$$

$$present[i] = present[i] + v[i] \quad (7)$$

$v[i]$ is the particle velocity, $present[i]$ is the current particle (solution), $pbest[i]$ and $gbest[i]$ are defined as stated before, $rand(i)$ is a random number between (0,1) and $c1, c2$ are learning factors. Usually $c1=c2=2$.

4.1.4. Implementation of PSO for tetrolet-based segmentation :

The implementation of the segmentation algorithm consists of the following steps.

Step 1: Swarm Formation: For a population size p , the particles are randomly generated between the minimum and the maximum limits of the threshold values.

Step 2: Objective Function evaluation: The objective function values of the particles are evaluated.

Step 3: 'pbest' and 'gbest' initialization: The objective values obtained above for the initial particles of the swarm are set as the initial $pbest$ values of the particles. The best value among all the $pbest$ values is identified as $gbest$.

Step 4: Velocity computation: The new velocity for each particle is computed using equation (6).

Step 5: Position computation: The new position for each particle is computed using equation (7).

Step 6: Swarm Updation: The values of the objective function are calculated for the updated positions of the particles. If the new value is better than the previous $pbest$, the new value is set to $pbest$. Similarly, $gbest$ value is also updated as the best $pbest$.

Step 7: Termination: If the stopping criteria are met, the positions of particles represented by $gbest$ are the

optimal threshold values. Otherwise, the procedure is repeated from step 4.

Fig. 5 provides a snapshot of the input, edge detected and the segmented images.

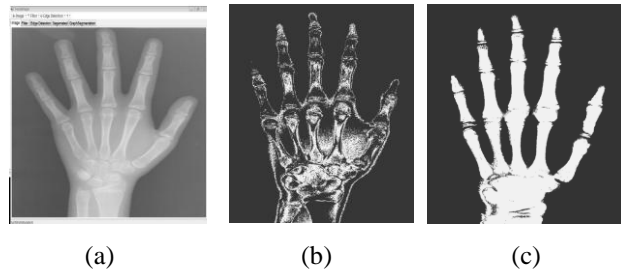


Fig. 5. (a) Pre-processed image (b) Edge detected image (c) Segmented image

4.2 Feature Extraction and Analysis

Feature extraction is performed as a way to reduce the dimensionality of the data. A long list of candidate features was calculated in order to form a powerful input vector. The features attempted to describe the morphology of the outline shape of the bones (ROIs). Once extracted and optimized, the vector would be used to train and validate the classifier. The list of candidate features are categorized into two groups, based on the ROIs they are extracted from, as:

1. Carpal features: (9 features)
 - *BRlength*
 - *BRwidth*
 - *BRdiagonal*
 - *BRarea*
 - *BRperimeter*
 - *INarea*
 - *INperimeter*
 - *BR_INratio*
 - *Solidity*
2. Phalangeal features: (3 + 12 x 3 + 3 =42)
 - *MedianLength* (3 fingers)
 - *DistalValues* (3 fingers)
 - *DistalLength*
 - *DistalWidth*
 - *DistalArea*
 - *DistalPerimeter*
 - *MiddleValues* (3 fingers)
 - *MiddleLength*
 - *MiddleWidth*
 - *MiddleArea*
 - *MiddlePerimeter*
 - *ProximalValues* (3 fingers)
 - *ProximalLength*
 - *ProximalWidth*
 - *ProximalArea*
 - *ProximalPerimeter*

- *DA/DP* – Average of the ratios of *DistalArea* and *DistalPerimeter* of the three fingers.
- *MA/MP* – Average of the ratios of *MiddleArea* and *MiddlePerimeter* of the three fingers.
- *PA/PP* – Average of the ratios of *ProximalArea* and *ProximalPerimeter* of the three fingers.

4.2.1. *Carpal Features:*

For the carpal bones, all the carpal bones are together identified as an inner region and are enclosed inside a bounding rectangle. Five features, namely the length, width, area, perimeter and the diagonal length of the bounding rectangle are calculated. The length and width are calculated as the sum of pixels along the boundary.

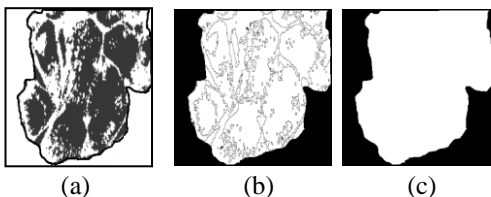


Fig. 6. (a) Carpal ROI (b) Region Fill (c) Inner region

The area, perimeter and diagonal are given by,

$$Area = Length \times Width \tag{8}$$

$$Perimeter = 2 \times Length + 2 \times Width \tag{9}$$

$$Diagonal = \sqrt{Length^2 + Width^2} \tag{10}$$

For the inner region of carpals, two features namely the inner area and perimeter are calculated as the number of pixels enclosed within the boundaries, and along the boundaries of the sample region respectively. The next carpal feature is the ratio between the outer and inner areas given by,

$$BR_INratio = \frac{BRarea}{INarea} \tag{11}$$

Solidity, the last carpal feature is defined as the number of pixels in the foreground, which quantifies the solidity of the carpal bones identified. Thus, a total of 9 carpal features are extracted. Fig. 6 provides the snapshot of extracting the carpal ROI features.

4.2.2. *Phalangeal Features:*

Phalangeal features are extracted from three fingers, namely the index, middle and third finger. For each finger, the three phalangeal bones: distal, middle

and proximal are considered and from each of them four features are extracted (length, width, area, perimeter). Also the length of the median for the finger phalanges is calculated for each finger. The ratio of the area and perimeter for the distal, middle and proximal phalanges of the three fingers are calculated and averaged to obtain 3 features, *DA/DP*, *MA/MP* and *PA/PP*. Thus, a total of 42 features are extracted from the phalangeal bones. Fig. 7 provides the snapshot of extracting and cropping the phalangeal ROI. Fig. 8. (a) shows the extraction of features from the distal, middle and proximal phalanges individually and (b) shows the extraction of *MedianLength* feature.

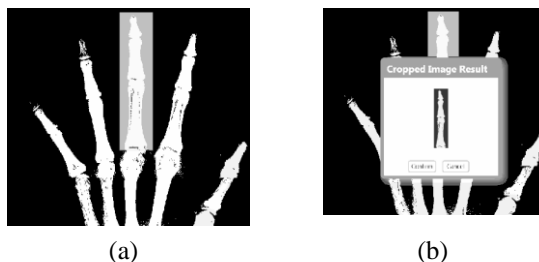


Fig. 7. (a) Phalangeal ROI (b) Cropped region



Fig. 8. (a) Identifying distal, middle and proximal ROI (b) Extracting Length of median

4.2.3. *Feature Analysis:*

Totally 51 features are extracted from the segmented bones of the left hand wrist radiograph, producing a multi-dimensional set of data. The exploration of the data set can give a valuable insight of the expected behavior of the end system and therefore assist further improvement of its performance [44]. But the great number of features defined and computed makes it impossible to use them all in classification. Also, redundant inputs may degrade the overall performance of the classifier. Thus, the need for a feature selection procedure is very evident. In the proposed system, Principal Component Analysis (PCA) is employed for dimensionality reduction. The extracted features are analyzed using PCA, thus reducing the feature vector into 11 important features. PCA [45-47] is a vector space transformation often used to reduce multidimensional datasets to lower dimensions for analysis. Given data *X* consisting of *N* samples, PCA first performs data normalization by subtracting the mean vector *m* from the data. Then the covariance matrix Σ of the normalized data (*X* - *m*) is computed.

$$m = \frac{1}{N} \sum_{i=1}^N X_i \tag{12}$$

$$\Sigma = (X - m)(X - m)^T \tag{13}$$

Afterwards, the basis functions are obtained by solving the algebraic eigen value problem

$$\Lambda = \Phi^T \Sigma \Phi \tag{14}$$

where Φ is the eigenvector matrix of Σ , and Λ is the corresponding diagonal matrix of eigen values. Feature selection is then performed by keeping q ($q < N$) orthonormal eigen vectors corresponding to the first q largest eigen values of the covariance matrix.

4.2.4. Feature Selection:

The features that dominate the others in feature analysis are found to be the principal components. Those features are selected for further processing, discarding the lagging ones. The first seven predominant features selected in our system are: *BRperimeter*, *Solidity*, *BR_INratio*, *MedianLength*, *DA/DP*, *MA/MP*, and *PA/PP*. Thus the feature vector is reduced from 51 features to 7 features that contribute best in the bone age estimation process. The discrimination power of the selected features is depicted by plotting them against the estimated bone age, shown in Fig. 9. From the plots, the following are inferred:

- The carpal features contribute more during the earlier classes of the age group 1-10, while phalangeal features contribute much during the latter classes.
- The growth of carpal bones seems to be more rapid in girls, while it is gradual and slow in boys.
- The growth of the phalangeal bones is gradual both in boys and girls, at the same time their growth seem to be dominant in boys rather than in girls.
- When considering similarity, the *MedianLength* feature from the phalanges showed similar values for boys and girls.
- Much difference is encountered between boys and girls in the ossification of the distal phalanges, thus showing significant disparity in the feature *DA/DP*.

4.3 Skeletal Age Inference

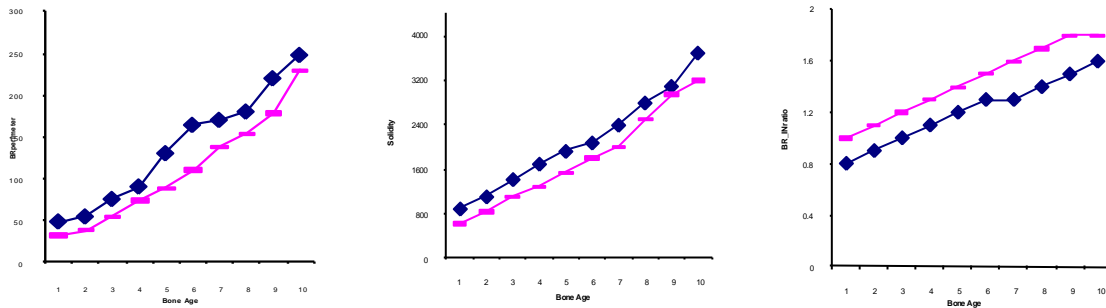
This module is responsible for translating the features into corresponding skeletal bone age. The selected features after analysis cannot be directly used for age estimation. So they are modeled into a suitable format for further analysis.

4.3.1 Feature Modeling:

The selected features are modeled into more formal features to make them suitable for processing and classification. The features are modeled based on their values corresponding to age, to fall between the classes A to J in normal cases. If they are below the lower threshold bound T_L , they are classified to class Z and if they are above the higher threshold bound T_H , they are classified to class X. The criteria selection for the features is given in Table 1. Each of the selected 7 features is modeled into any of the above mentioned categories, based on their values, v in years. After framing the formal features, classification is done using the renowned ID3 classifier.

Table 1. Criteria Selection

S.No.	Category	Values v (Years)
1.	Z	$v < T_L$
2.	A	$T_L < v < 1$ year
3.	B	1 year $< v < 2$ year
4.	C	2 year $< v < 3$ year
5.	D	3 year $< v < 4$ year
6.	E	4 year $< v < 5$ year
7.	F	5 year $< v < 6$ year
8.	G	6 year $< v < 7$ year
9.	H	7 year $< v < 8$ year
10.	I	8 year $< v < 9$ year
11.	J	9 year $< v < T_H$
12.	X	$v > T_H$



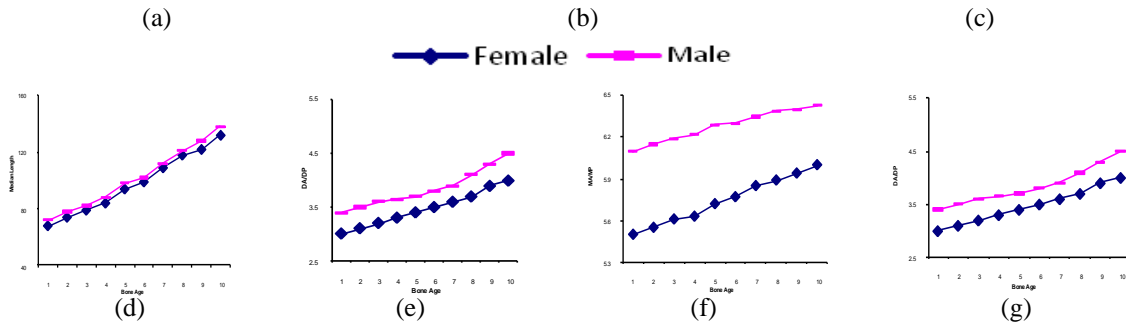


Fig. 9. Selected Features Vs Estimated Bone age (a)BRperimeter (b)Solidity (c)BR_INratio (d)MedianLength (e)DA/DP (f)MA/MP (g)PA/PP.

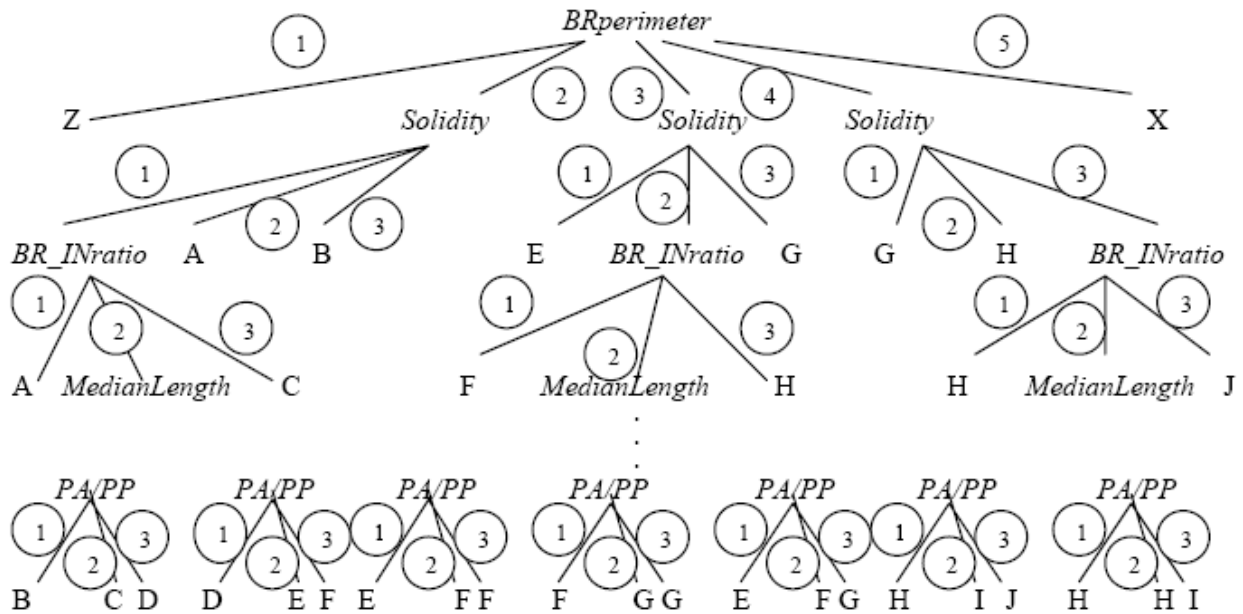


Fig. 10. ID3 Decision Tree

4.3.2. ID3 classifier:

Studies reveal that there may be discrepancies in the results of classifications by different radiologists or at sometimes even between the classifications by the same radiologist in different moments [48]. This is because some stages are mistaken with the nearby stages easily. So it becomes difficult to strictly define the features. Instead, they have a certain degree of overlapping between them, since the growth pattern is gradual. Also the features can fall into only any one of the categories (i.e.) mutually exclusive. So the ID3 classifier is more suitable for the BAA system. The root of the ID3 tree is formed with the feature *BRperimeter*, followed by *Solidity*, *BR_INratio*, *MedianLength*, and so on. We have given more importance to the carpal features than those from the phalanges because the features from the carpal bones influence more the

estimation process for the age group 1-10. Hence carpal features form the root and higher level nodes of the ID3 decision tree, followed by the phalangeal features. To avoid complexity, only selected layers of the ID3 tree are depicted in Fig. 10. The inputs to the tree will be the 7 features modeled as values in years, and the output will be the skeletal class or category. The selected class is then mapped onto the skeletal bone age.

4.3.3. Training Sets:

The ID3 decision tree was trained with 6 male and 6 female radiographs for each age group, thus with a total of 120 radiographs, 60 male and 60 female cases for the age group 1-10. After the decision tree was built and fine-tuned [49,50], 50 radiographs from girls and 50 from boys were used to test it. The results showed that 43 out of 50 were correctly classified for the girls (86%) and 42 out of 50 were correctly classified for the boys

(84%). The classification error was to assign a later class or a previous class.

Results and Discussion

The performance of the BAA system in estimating the bone age of patients was evaluated using a dataset consisting of 100 digital radiographs (50 for boys and 50 for girls). The quality of the image is a vital factor of influence in the estimation process. So much consideration was imparted on obtaining quality radiographs. Also particular attention was dedicated to design and implement robust techniques for preprocessing and reliable feature extraction. During the preprocessing, the noise caused due to radiation and other external factors were eliminated. The accuracy of segmentation was measured using the number of under selected and over selected pixels. The segmentation was regarded as accurate if the sum of over selected and under selected pixels were less than 25. The segmentation process was accurate by 94% for boys and 96% for girls, as tabulated in Table 1. From the segmented ROI, 9 carpal and 42 phalangeal features were extracted. The feature extraction process was evaluated based on the measurability, ease of measuring, and the reliability of the feature data such as area and perimeter. The accuracy of feature extraction from the carpal and phalangeal bones is shown in Table 2. The ease and accuracy of feature extraction for the

proximal phalanges and the inner carpal area were slightly imprecise when compared to the other features, the reason being that these bones were comparatively interior. Also in some of the radiographs, the zones where the phalanges are located are dark with low contrast. Feature space reduction was done using PCA. The contribution of each selected feature towards bone age estimation was correlated by plots (refer Fig. 11). Finally ID3 classifier was used to estimate the final bone age. The accuracy of the classifier was measured in terms of perfection in classification rate. Classification rate, CR is defined as the ratio of the number of correctly classified images N_{CC} to the total number of test images input to the classifier, N_{IP} .

$$CR = \frac{N_{CC}}{N_{IP}} \quad (15)$$

Incorrectly classified images include the images with under estimated or over estimated bone age when compared with the bone age estimated by a radiologist expert. For the correct classification, a tolerance limit ToL of 1 year more or less was considered negligible (i.e. $ToL = \pm 1 \text{ year}$). The accuracy of classification is given in Table 3. The proposed bone age estimation system was accurate in estimating the bone age of boys by 84% and girls by 86%.

Table 1. Accuracy of Segmentation

	No. of Images	Accurate	Inaccurate	Accuracy
Boys	50	47	3	94%
Girls	50	48	2	96%

Table 2. Accuracy of Feature Extraction

	BR (Outer)	Carpal (Inner)	Distal	Middle	Proximal
Area	100%	86%	98%	96%	90%
Perimeter	100%	82%	96%	95%	88%

Table 3. Accuracy of Classification

	No. of Images	Accurate Perfectly	Accurate (< ToL)	Inaccurate (> ToL)	Accuracy
Boys	50	40	2	8	84%
Girls	50	42	1	2	86%

Conclusions and Future work

The work presents an efficient system for skeletal age assessment. The system takes digital left hand wrist radiographs as input and outputs the skeletal bone age as the output. There are two phases: the training phase and the testing phase. The former is used to build and fine tune the ID3 decision tree classifier and the latter is

used to estimate the bone age. The input images were first preprocessed by smoothening with Gaussian filter. Then edges of the bones were detected using Sobel operator and segmentation was done by a new PSO algorithm using Tetrolets. From the segmented ROI, 9 carpal features and 42 phalangeal features were extracted. The extracted features were analyzed using

PCA and among them 7 dominant features were selected. Feature modeling was done to convert the selected features into a form understandable by the classifier. The ID3 classifier mapped the features onto the bone age class for the image. This bone age class disguised the bone age. The system was tested on a set of 100 radiographs (50 from girls and 50 from boys), achieving a success rate for bone age estimation of 86% for girls and 84% for boys. Future work will be focused on extending the system to work on the age group above 10 years, broadening the system to include the further TW2 bones such as radius, ulna, etc. and integrating the system with PACS.

References:

- [1] Vicente Gilsanz, and Osman Ratib, *Hand Bone Age – A Digital Atlas of Skeletal Maturity*, Springer-Verlag, 2005.
- [2] Concetto Spampinato, “Skeletal Bone Age Assessment”, University of Catania, Viale Andrea Doria, 6 95125, 1995.
- [3] R.K.Bull, P.D.Edwards, P.M.Kemp, S.Fry, I.A.Hughes, “Bone Age Assessment: a large scale comparison of the Greulich and Pyle, and Tanner and Whitehouse (TW2) methods, *Arch. Dis. Child*, vol.81, pp. 172-173, 1999.
- [4] J.M.Tanner, R.H.Whitehouse, *Assessment of Skeletal Maturity and Prediction of Adult Height (TW2 method)*, Academic Press, 1975.
- [5] Sankar K. Pal, and Robert A. King, “On Edge Detection of X-Ray Images using Fuzzy Sets”, *IEEE Trans. on Pattern Analysis and Machine Intelligence*, vol.5, no.1, pp.69-77, 1983.
- [6] A.Kwabwe, S.K.Pal, R.A.King, “Recognition of bones from rays of the hand”, *International journal of Systems and Science*, 16(4): 403-413, 1985.
- [7] Amita Pathak, S.K.Pal, “Fuzzy Grammars in Syntactic Recognition of Skeletal Maturity from X-Rays”, *IEEE Trans. on Systems, Man, and Cybernetics*, vol.16, no.5, 1986.
- [8] David J. Michael, Alan C. Nelson, “HANDX: A Model-Based System for Automatic Segmentation of Bones from Digital Hand Radiographs”, *IEEE Trans. on Medical Imaging*, vol.8, no.1, 1989.
- [9] E. Pietka, M. F. McNitt-Gray, and H. K. Huang, “Computer-assisted phalangeal analysis in skeletal age assessment,” *IEEE Trans. Med. Imag.*, vol. 10, pp. 616–620, 1991.
- [10] S. M. Garn, K. P. Hertzog, A. K. Poznanski, and J. M. Nagy, “Metacarpophalangeal length in the evaluation of skeletal malformation,” *Radiology*, vol. 105, pp. 375-381, 1972.
- [11] J. M. Tanner and R. D. Gibbons, “Automatic bone age measurement using computerized image analysis,” *J. Ped. Endocrinol.*, vol. 7, pp. 141–145, 1994.
- [12] E. Pietka, L. Kaabi, M. L. Kuo, and H. K. Huang, “Feature extraction in carpal-bone analysis,” *IEEE Trans. Med. Imag.*, vol. 12, pp. 44–49, 1993.
- [13] S.N.C.Cheng, H.Chen, L.T.Niklason, R.S.Alder, “Automated segmentation of regions on hand radiographs”, *Med. Phy.*, vol. 21, pp.1293-1300, 1994.
- [14] N.M.Drayer and L.A.Cox, “Assessment of bone ages by the Tanner-Whitehouse method using a computer-aided system, *Acta Paediatric Suppl.*, pp.77-80, 1994.
- [15] Al-Taani, A.T., Ricketts, I.W., Cairns, A.Y., “Classification Of Hand Bones For Bone Age Assessment”, *Proceedings of the Third IEEE International Conference on Electronics, Circuits, and Systems, ICECS '96.*, pp.1088-1091, 1996.
- [16] Wastl, S., Dickhaus, H. : “Computerized Classification of Maturity Stages of Hand Bones of Children and Juveniles”, *Proceedings of 18th IEEE International Conference EMBS*, pp.1155-1156, 1996.
- [17] Mahmoodi, S., Sharif, B.S., Chester, E.G., Owen, J.P., Lee, R.E.J.: “Automated vision system for skeletal age assessment using knowledge based techniques.” *IEEE conference publication*, ISSN 0537-9989, issue 443: 809–813, 1997.
- [18] E. Pietka, A. Gertych, S. Pospiech, F. Cao, H. K. Huang, and V. Gilsanz, “Computer-assisted bone age assessment: Image preprocessing and epiphyseal/ metaphyseal ROI extraction,” *IEEE Trans. Med. Imag.*, vol. 20, no. 8, pp. 715–729, Aug. 2001.
- [19] M. Niemeijer, B. van Ginneken, C. Maas, F. Beek, and M. Viergever, “Assessing the skeletal age from a hand radiograph: Automating the Tanner-Whitehouse method,” in *Proc.Med. Imaging, SPIE*, vol. 5032, pp. 1197–1205, 2003.
- [20] T. F. Cootes, A. Hill, C. J. Taylor, and J. Haslam, “The Use of Active Shape Models for Locating Structures in Medical Images,” in *Proceedings of 13th Int. Conf. on IPMI*, (London, UK), pp. 33–47, Springer-Verlag, 1993.
- [21] Miguel A. Martin-Fernandez, Marcos Martin-Fernandez, Carlos Alberola-Lopez, “Automatic bone age assessment: a registration approach”, *Medical Imaging 2003: Image Processing, Proceedings of SPIE*, vol. 5032, pp. 1765-1776, 2003.
- [22] Santiago Aja-Fernandez, Rodrigo de Luis-Garcia, Miguel Angel Martin-Fernandez, Carlos Alberola-Lopez, “ A computational TW3 classifier for

- skeletal maturity assessment: A Computing with Words approach”, *Journal of Biomedical Informatics*, vol. 37, no.2, pp. 99–107, 2004.
- [23] R. de Luis, M. Martin, J. I. Arribas, and C. Alberola, “A fully automatic algorithm for contour detection of bones in hand radiographies using active contours,” *Proc. IEEE Int. Conf. Image Process.*, vol. 2, pp. 421-424, 2003.
- [24] Pan Lin, Feng Zhang, Yong Yang, Chong-Xun Zheng, “Carpal-Bone Feature Extraction Analysis in Skeletal Age Assessment Based on Deformable Model”, *Journal of Computer Science and Technology*, vol. 4, no. 3, pp. 152-156, 2004.
- [25] A. Tristan-Vega and J. I. Arribas, “A radius and ulna TW3 bone age assessment system,” *IEEE Trans Biomed Eng.*, vol. 55, pp. 1463–1476, 2008.
- [26] A. Zhang, A. Gertych, B. Liu, “Automatic bone age assessment for young children from newborn to 7-year-old using carpal bones”, *Computerized Medical Imaging and Graphics*, vol. 31, Issue 4 - 5, pp. 299 – 310, 2007.
- [27] H. Thodberg, S. Kreiborg, A. Juul, and K. Pedersen, “The Bone Xpert Method for Automated Determination of Skeletal Maturity”, *IEEE Trans Med Imaging*, vol. 28, no. 1, pp. 52–66, 2009.
- [28] D. Giordano, R. Leonardi, F. Maiorana, G. Scarciofalo, and C. Spampinato, “Epiphysis and Metaphysis Extraction and Classification by Adaptive Thresholding and Dog Filtering for Automated Skeletal Bone Age Analysis,” in *Proc. of the 29th Conference on IEEE Engineering in Medicine and Biology Society*, pp. 6551–6556, 2007.
- [29] Chi-Wen Hsieh, Tai-Lang Jong, Yi-Hong Chou and Chui-Mei Tiu, “Computerized geometric features of carpal bone for bone age estimation”, *Chinese Medical Journal*, 120(9):767-770, 2007.
- [30] Zhao Liu, Jian Liu, Jianxun Chen, Linqun Yang, “Automatic Bone Age Assessment Based on PSO”, *IEEE*, 2007.
- [31] D. Giordano, C. Spampinato, G. Scarciofalo, R. Leonardi, “An Automatic System for Skeletal Bone Age Measurement by Robust Processing of Carpal and Epiphysal/Metaphysal Bones” *IEEE Trans. On Instrumentation and Measurement*, vol.59, issue 10, pp. 2539-2553, 2010.
- [32] P.Thangam, K.Thanushkodi, T.V.Mahendiran, “Skeletal Bone Age Assessment – Research Directions”, *International Journal of Advanced Research in Computer Science*, vol. 2, No. 5, pp. 415 – 423, 2011.
- [33] P.Thangam, K.Thanushkodi, T.V.Mahendiran, “Computerized Convex Hull Method of Skeletal Bone Age Assessment from Carpal Bones”, *European Journal of Scientific Research*, Vol.70 No.3, pp. 334-344, 2012.
- [34] P.Thangam, K.Thanushkodi, T.V.Mahendiran, “Efficient Skeletal Bone Age Estimation Method using Carpal and Radius Bone features”, *Journal of Scientific and Industrial Research*, Vol. 71, No. 7, July 2012.
- [35] P.Thangam, K.Thanushkodi, T.V.Mahendiran, “Computerized Skeletal Bone Age Assessment from Radius and Ulna bones”, *International Journal of Systems, Applications and Algorithms*, Vol. 2, Issue 5, May 2012.
- [36] P.Thangam, K.Thanushkodi, T.V.Mahendiran, “Skeletal Bone Age Assessment from Epiphysis/Metaphysis of phalanges using Hausdorff distance”, *Scientific Research and Essays*, Vol. 7, No. 28, pp. 2495-2503, 2012.
- [37] Rafael C.Gonzalez, Richard E. Woods, *Digital Image Processing*, Third Edition, (Pearson, 2009).
- [38] Jens Krommweh, Tetrolet Transform: A New Adaptive Haar Wavelet Algorithm for Sparse Image Representation”, *J.Vis. Commun.* (2010), doi:10.1016/j.jvcir.2010.02.011.
- [39] J. Kennedy, and R.C. Eberhart, “Particle Swarm Optimization,” *Proc of the IEEE International Conference on Neural Networks*, Australia, pp. 1942–1948. 1995.
- [40] J.Kennedy, R.C.Eberhart, Y.Shi, *Swarm Intelligence*, Morgan Kaufmann Publishers, 2001.
- [41] Nadia Nedjah, Luiza de Macedo Mourelle, *Swarm Intelligent Systems*, Springer, 2006.
- [42] <http://www.swarmintelligence.org/>
- [43] <http://www.particleswarm.info/>
- [44] Lefkaditis, D., Awcock, G. J. & Howlett, R. J., Intelligent Optical Otolith Classification for Species Recognition of Bony Fish, in *International Conference on Knowledge-Based & Intelligent Information & Engineering Systems*, Bournemouth, UK: Springer-Verlag, pp. 1226-1233, 2006.
- [45] Lindsay I Smith, *A Tutorial on Principal Component Analysis*, Feb 2002.
- [46] Christopher J.C. Burges, *Geometric Methods for Feature Extraction and Dimensional Reduction*, (Microsoft Research).
- [47] Mark S. Nixon and Alberto S. Aguado, *Feature Extraction and Image Processing*, (Newnes, 2002).
- [48] Vinuela-Rueda B, Alberola-Lopez S, “Inter and intra observer variability in bone age assessment using TW2-RUS”, In: *26 Congreso Nacional Soc. Esp. Rad. Medica*, Maspalomas, Spain; 2002.

-
- [49] Bing Liu, Yiyuan Xia, and Philip S. Yu, "Clustering through decision tree construction", *Proceedings of the ninth international conference on Information and knowledge management*, ACM, New York, 2000.
- [50] Richard O.Duda, Peter E.Hart and David G.Stork, *Pattern Classification*, Second Edition, John Wiley, 2002.